Proceedings of the 25th International Conference on
Port and Ocean Engineering under Arctic Conditions
June 9-13, 2019, Delft, The Netherlands

Medium-scale consolidation of artificial ice ridge – Part I: surface temperature, thickness and mechanical properties

Evgenii Salganik[1,2], Knut Vilhelm Høyland[1], Aleksey Shestov[2], Sveinung Løset[1], Anne-Niekolai Heijkoop[2,3]

[1] Sustainable Arctic Marine and Coastal Technology (SAMCoT), Centre for Research-based Innovations (CRI), Norwegian University of Science and Technology, Trondheim, Norway
[2] The University Centre in Svalbard, Longyearbyen, Norway
[3] Delft University of Technology, Delft, Netherlands

ABSTRACT

This paper is describing preparations and methods of medium-scale ridge consolidation experiment and development of ridge and surrounding level ice morphological, thermal, and mechanical characteristics for the experiment, performed in 2017 in Svalbard. It is also providing analysis and modelling of freezing rates and surface temperatures.

In February–May of 2017 for 66 days, experiment on ice ridge consolidation was performed in seawater Vallunden Lake connected with Van Mijen Fjord. 55 ice blocks were cut from level ice of 50 cm thickness and placed into the open water basin of 4.9 m by 3.0 m. Both level ice and artificial ridge were equipped with temperature sensors. During 3 visits, manual measurements of uniaxial strength in vertical and horizontal directions, salinity, gas volume, ice and snow thickness were performed for both level ice and ridge consolidated layer. 42 level ice and 25 ridge small-scale compression tests were completed in situ and in laboratory conditions.

The surface temperature of level ice was significantly warmer than of the ridge during most of the experiment, while the average snow thickness was higher for the ridge. During the experiment, 717°Cd were accumulated, and level ice grew from 50 cm up to 99 cm while the consolidated layer grew up to 120 cm. The analysis of the difference in consolidated layer thickness from temperature profiles in the ridge voids and blocks is given. The uniaxial compressive strength of the consolidated layer was between vertical and horizontal level ice strength for both in situ and laboratory tests.

KEY WORDS: Ice; Ridges; Solidification; Thermodynamics; Fieldwork.

NOMENCLATURE

c_b Specific heat capacity of the brine [Jkg^{-1}K^{-1}]

c_i Specific heat capacity of the ice [Jkg^{-1}K^{-1}]

h_i Ice thickness [m]

h_s Snow thickness [m]

h_{si} Sea ice thickness [m]

k_i Thermal conductivity of the ice [Wm^{-1}K^{-1}]

k_s Thermal conductivity of the snow [Wm^{-1}K^{-1}]

m_i Mass fraction of ice

q Heat flux [W/m^2]

H_{ia} Air convectional heat transfer coefficient [Wm^{-2}K^{-1}]

H_{si} Specific sea ice enthalpy [J/kg]

L_i Specific latent heat of pure ice [J/kg]

S_i Bulk salinity of ice [°C]

T_a Air ambient temperature [°C]

T_{as} Air-snow interface temperature [°C]

T_f Water freezing temperature [°C]

T_{si} Snow-ice interface temperature [°C]

η_t Ridge total porosity

ρ_i Pure ice density [kg/m^3]

ρ_{si} Sea ice density [kg/m^3]

INTRODUCTION

According to the definition of the WMO (1970), an ice ridge is a line or wall of broken ice forced up by pressure. Ridges usually consist of three parts: the sail, the consolidated layer, and the unconsolidated rubble. A significant part of loads on offshore structures and vessels is coming from the consolidated layer (Ervik et al., 2019). Høyland (2002) defined three phases of ridge consolidation: initial, main and decay. End of the initial phase is when the unconsolidated part is at the water freezing temperature. The thickness of level ice and the consolidated layer is the main value of interest for structural loads. It can be measured by mechanical drilling or from vertical temperature profile.

There are only several ridge consolidation models (Leppäranta et al., 1995), confirmed by observations with accurately measured conditions and initial parameters. Seasonal development of consolidated layer was described by Blanchet (1998), Høyland (2002), and Shestov et al. (2018).

Timco and Goodrich (1988), and Salganik and Høyland (2018) provided data about basin-scale experiments in ridge consolidation. Meanwhile, small-scale experiments cannot provide confidence in large-scale models due to the significant difference in the importance of separate mechanisms of heat transfer and significant simplifications in laboratories including the absence of snow. Ashton (1989) showed the difference between thin and thick fresh ice growth.

The consolidated layer is usually growing from the initial phase with zero minimum ice thickness until thicknesses larger than of surrounding ice. This means that ridge solidification includes a large range of scales and ratios of thermal resistances.

The consolidation process is usually characterized by the ratio of the consolidated layer and level ice thicknesses called a degree of consolidation. Natural ridging process can occur at

any time throughout the season. This makes the ratio of the number of cold days when level ice and consolidated layer are growing random. The common way to describe ridge consolidation via its degree of consolidation is practical for engineering purposes, but not so useful for solidification model validation due to sensitivity to the initial level ice thickness at the moment of ridging.

Medium-scale solidification experiments are providing the unique advantage of accurately measured parameters such as initial macro-porosity, initial block temperature and salinity, and freezing time. It minimizes error in key parameters for the solidification process, which includes air natural and forced convection, conduction through snow and ice, and phase change. Saline ice is a composite material, so any temperature or salinity change leads to the change of sea ice solid fraction. In natural conditions, solidification includes also warming, described by Shestov et al. (2018). In this paper, we are trying to define and validate a simple analytical solidification model suitable for transient air temperature, wind speed, and snow thickness. The aim of the field experiment was to compare thermodynamics and development of physical and mechanical parameters of level ice and consolidated layer.

Level ice growth in steady-state conditions depends on how the temperature difference between air and water is distributed between insulating layers of air, snow, and ice. For slow changes of boundary conditions, the temperature gradient at the bottom of ice depends on the ice top surface temperature and its thickness. Three thermal resistances define temperature profile and the total system thermal resistance is showing how much heat can be transported in time from the water to the air:

$$q = \frac{T_a - T_{as}}{R_a} = \frac{T_{as} - T_{si}}{R_s} = \frac{T_{si} - T_f}{R_i} = \frac{T_a - T_f}{R_a + R_s + R_i};$$ (1)

$$R_a = 1/H_{ia};$$ (2)

$$R_s = h_s/k_s;$$ (3)

$$R_i = h_i/k_i;$$ (4)

In transient conditions, temperature distribution will be following described ratios with a time lag defined by the thermal inertia of snow and ice. Thermal inertia for saline ice can be divided into specific heat of pure ice and brine, and change of solid fraction at different temperatures, which requires freezing or melting of pure ice inside sea ice. The sum of both effects can be presented via the enthalpy of sea ice:

$$H_{si} = -L_i m_i - m_i \int c_i dT - (1 - m_i) \int c_b dT$$ (5)

Enthalpy values at different temperatures illustrate the difference from simplified ice growth known as Stefan equation of ice growth: depending on ice temperature and salinity only a certain mass fraction should be frozen, while additional negative heat should be spent to adjust ice temperature to a certain temperature profile. Zero value of enthalpy can be chosen arbitrarily and assumed zero at sea ice freezing point.

The enthalpy value for ice with any temperature and salinity distribution is defining how much energy should be extracted from the water for its solidification and cooling (Figure 1). As can be seen, enthalpy difference can be higher or lower than pure ice latent heat. Pure ice and brine sensible heat are decreasing sea ice growth at low temperatures in comparison to the Stefan equation. In contrast, the low solid fraction of warm sea ice can lead to faster growth in comparison to Stefan equation and pure ice growth. For salinity of 5 ppt warm ice at water freezing temperature requires 15 % less negative energy to be formed.
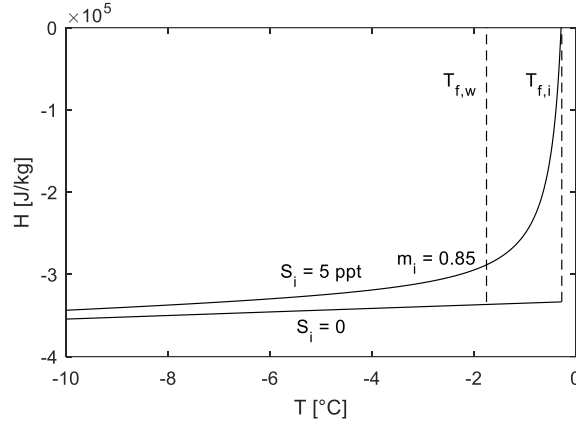
Figure 1. Saline and fresh ice enthalpy vs temperature.

The difference between the top and bottom heat fluxes in ice is spent on ice heating or cooling. When ice is thick enough, the bottom heat flux depends only on average top surface temperature.

Assuming no oceanic flux from the water, the pure ice growth can be estimated as:

$$\rho_i L_i \, dh_i/dt = -k_i \, \partial T/\partial z \tag{6}$$

Assuming no thermal inertia, the pure ice growth can be estimated from meteorological data including air temperature, wind speed, and snow thickness:

$$\rho_i L_i \frac{dh_i}{dt} = -k_i \frac{T_{si} - T_f}{h_i} = \frac{T_a - T_f}{R_a + R_s + R_i} \tag{7}$$

For the field data analysis, usage of the bottom ice boundary for heat flux calculation can be impractical due to high uncertainties in salinity and temperature profiles, while only the change of total ice volume is the main value of interest. According to Griewank and Notz (2013), different salinity profiles can change the ice growth prediction by less than 4 %. The thickness of saline ice including sensible heat can be estimated from pure ice thickness without sensible heat from the solid volume fraction as:

$$h_{si} = h_i \frac{\rho_i L_i}{\rho_{si} \Delta H_{si}} \tag{8}$$

This simple analytical model, which ignores time delay in thermal diffusion, can give errors when the air temperature is quickly moving towards seawater freezing point. This error can be eliminated only by solving diffusion equations for snow and saline ice layers assuming external convection from the air. The difference between analytical and numerical predictions will be presented in the results of this study.

Ridge consolidation has many similarities with level ice growth. Meanwhile, there are following critical differences: ridge is a porous media consisting out of 60–80 % of ice staying at the seawater freezing temperature under the bottom of the consolidated layer. Leppäranta and Hakala (1989) suggested considering this difference by assuming the value of ridge effective latent heat as:

$$L_r = \eta_t L_i \tag{9}$$

The vertical temperature gradient can be assumed homogeneous for ridges with small voids, but in natural scale, voids between ice blocks are in the range of consolidated layer thickness. Due to this inhomogeneity, horizontal heat fluxes are occurring inside ice ridges (Leppäranta et al., 1995), and ice-water interface has ellipse shape where new ice is forming (Petrich et al., 2007).

Another difference is the presence of large above water ice called sail in ice ridges, which is the locally changing ratio of thermal resistances and the total area via which heat is extracted to the air. The sail presence is caused by the trapezoidal shape of ridge keel and large underwater volume in comparison to level ice.

Ridge sail is also changing the distribution of snow, creating accumulations and snow-free surfaces. It is making top surface conduction to be a purely 3D problem in contrast to level ice. These factors are changing thermal resistance of ridge sail and its top surface temperature, making the analysis of field data much more complicated due to the difference in temperatures of different parts of the consolidated layer. Leppäranta et al. (1995) observed that the top of the ridge could be significantly colder while the sail temperature at the water level can be warmer than in sail free consolidated layer. Meanwhile, the 1D analytical model can be used for both void and block parts of the ridge, assuming the sum of these heat fluxes is spent for the new ice formation.

METHODS

The field experiment in the artificial ridge consolidation was performed during 66 days from 25 February 2017 until 4 May 2017 in Lake Vallunden in the Van Mijenfjorden in Svalbard. Lake Vallunden is a seawater lake connected with the seawater fjord by a small 100 m long channel (Marchenko and Morozov, 2013). The ridge was made of 55 blocks from 50 cm thick ice, totally 11.4 m^3 of ice. The average initial level ice salinity was 3.8 ppt (Figure 4a) and the average initial block temperature was -7.8°C. A basin 3.0 m by 4.9 m was made in the level ice cover, and the blocks were damped into this basin. The ice blocks were cut in the feeding channel using trencher (Figure 2a). After that, the blocks were placed into the water basin using rope, ramp, and snowmobile (Figure 2b).
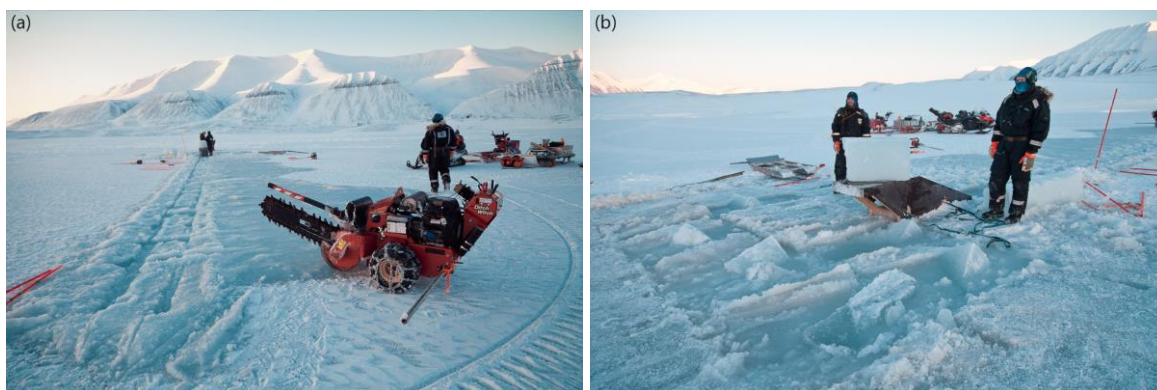

Figure 2. Feeding channel (a) and ridge formation using the ramp (b).

The following information was collected during 4 visits: temperature, salinity, density profiles, and uniaxial compressive strength. During the 1st visit 3 vertical cores were collected to investigate ridge morphology, and 12 vertical cores were collected at the 4th visit.

Both level ice and ridge were instrumented with thermistor strings. The ridge thermistor string was placed in the borehole 1 during the visit 1, the level ice thermistor was placed close to the ridge (Figure 3b). The top surface temperature of the ridge with 15 cm freeboard, the top surface temperature of level ice with 7 cm freeboard and air ambient temperature are shown at Figure 3a. Ice thickness was measured by drilling during 4 visits and was also estimated from vertical temperature profiles from thermistors (Figure 6a).

Sea ice thermodynamic parameters including heat capacity, thermal conductivity, latent heat and solid fraction were calculated from Notz (2005). Air convectional heat transfer coefficient as a function of the wind speed was estimated from Adams (1960), with the

average value for the time of experiment of 21 Wm^{-2}K^{-1}. Air ambient temperature and wind speed values were received from the Sveagruva meteorological station.
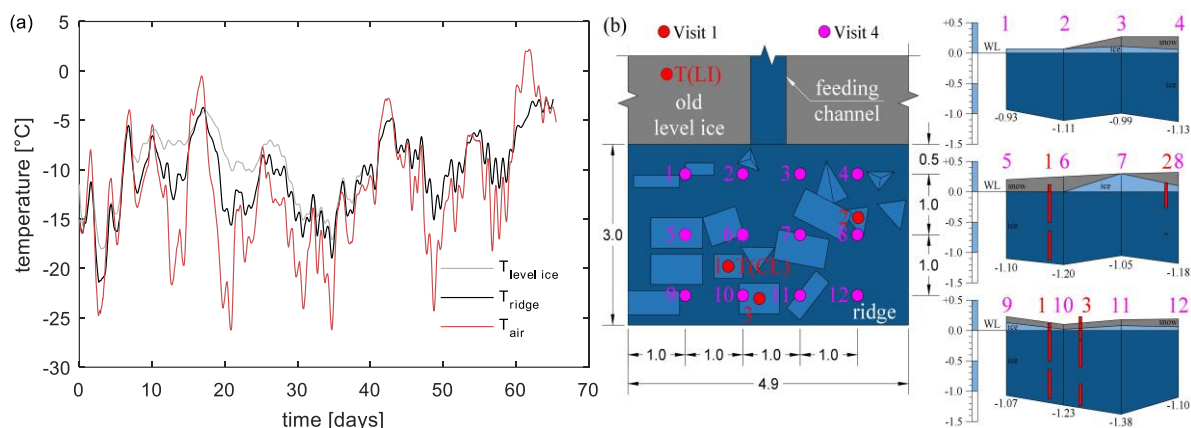

Figure 3. Air, level ice and ridge top surface temperatures (a) and ridge profiles (b)

Three cores were used to measure initial parameters of level ice from each the ridge was formed (Figure 4a). One core of the level ice and of the ridge were used for salinity and density profiles at the visit 4 (Figure 4b). The vertical resolution of salinity and density profiles was 5 cm.
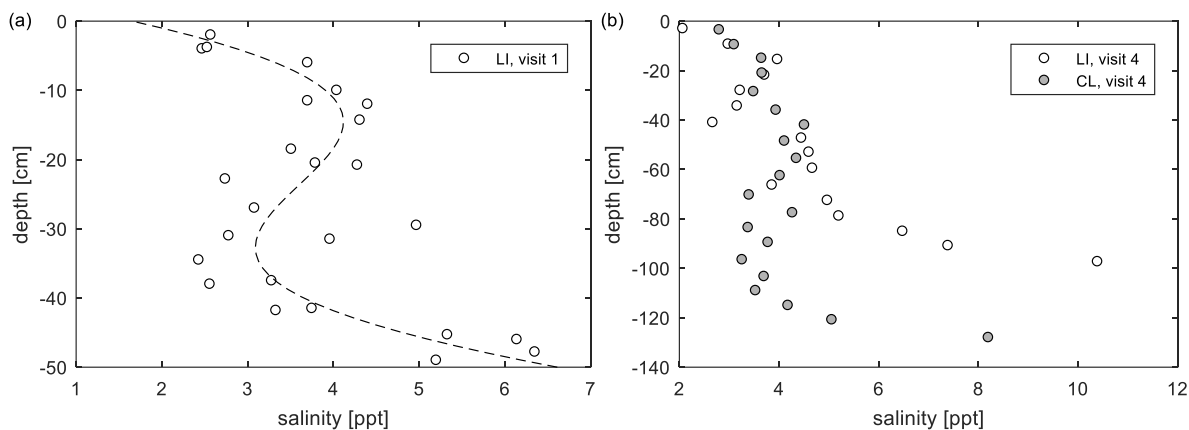

Figure 4. Salinity profiles for visit 1 (a) and for visit 4 (b).

12 vertical and horizontal level ice samples for uniaxial compression were collected during visit 2. 4 vertical level ice and 17 vertical ridge samples were also collected during visit 4. Tests with these samples were performed in the lab at a temperature near -10°C. 38 in-situ compression tests were performed during visit 3, including 32 for level ice and 6 for the ridge.

The numerical simulations of level ice and ridge consolidation were performed with finite element analysis simulation software COMSOL Multiphysics 5.3a using the front tracking method. The position of the ice-water boundary was defined by Stefan energy balance condition, where the difference of heat fluxes in two materials is equal to the amount of new solid formed or melted.

RESULTS

Brine volume (Figure 5a) was estimated for ice initial temperature and freezing temperature of the surrounding water in the formed ridge (Cox and Weeks, 1983). Ridge initial macro-porosity of 0.36 was estimated from the total volume of ice blocks, and from sail and keel elevations obtained from drilling (Figure 3b).
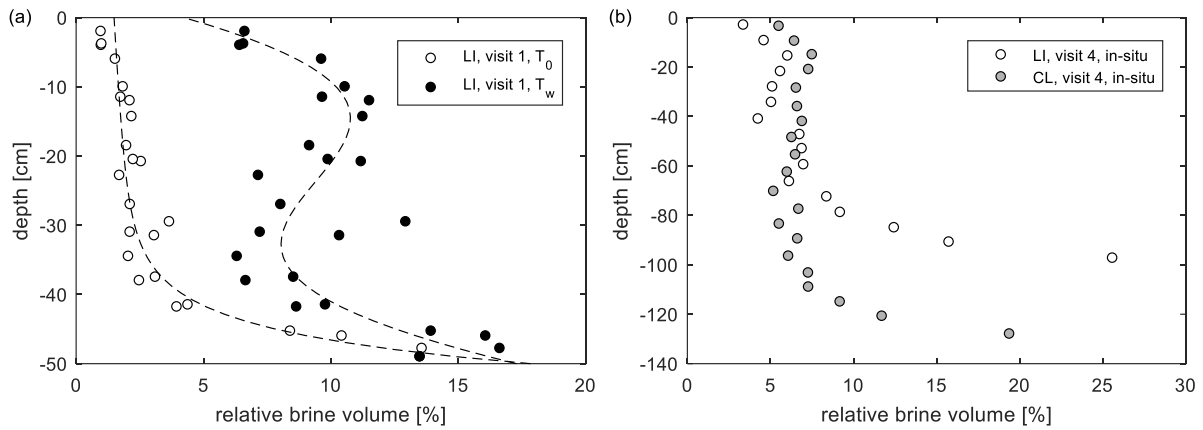
Figure 5. Relative brine volume profile for in-situ and water temperatures for visit 1 (a) and for visit 4 (b).

The average air temperature during consolidation experiment was -12.6°C from both meteorological station and upper sensor of the thermistor string. Average freeboard at visit 4 was 7 cm for level ice and 8 cm for the ridge. During the time of the experiment level ice grew from 50 cm to 99 cm, while the consolidated layer grew up to 120±12 cm (Figure 6a). The level ice salinity after 66 days changed from 3.8 ppt to 4.6 ppt, consolidated layer final salinity was 4.1 ppt (Figure 5b).
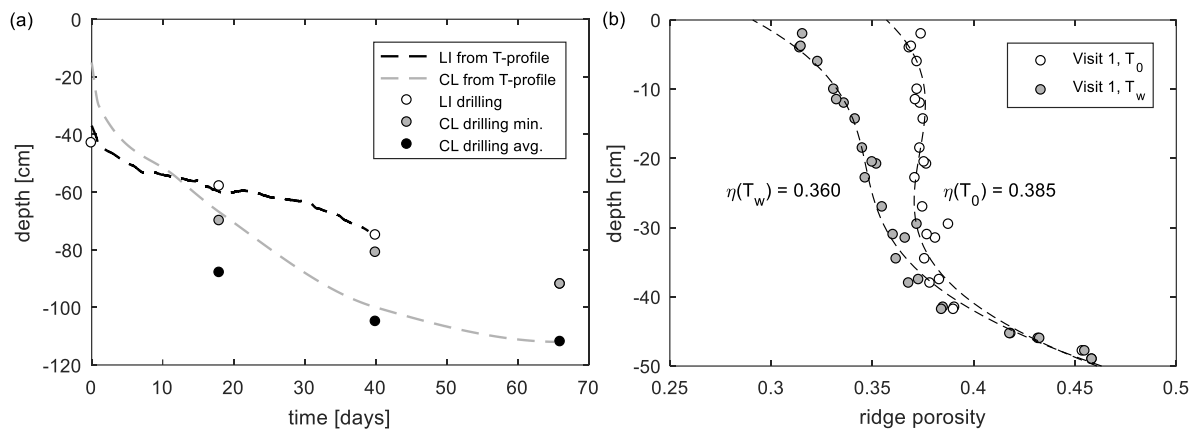

Figure 6. Ice thickness development (a) and ridge porosity profile before and after the initial phase of consolidation (b).

Due to block average initial temperature of -7.8°C, the ridge total porosity including brine and gas volumes should decrease from 0.39 to 0.36 under the assumption of salt conservation (Figure 6b).

The snow thermal conductivity value of $0.21\,Wm^{-2}$ was calculated from the level ice temperature profile to fit thermal resistance values for measured snow thickness (Figure 7a). Snow resistance values can be used for estimation of snow thermal conductivity for four visits when the snow thickness was measured. For the whole time of the experiment, the snow resistance data can show the exact time of snow thickness change. The snow thermal resistance above the ridge with 15 cm sail was 2.2 times lower than snow thermal resistance above level ice for measured snow thicknesses and the same snow thermal conductivity of $0.21\,W/m^2$ (Figure 7b).
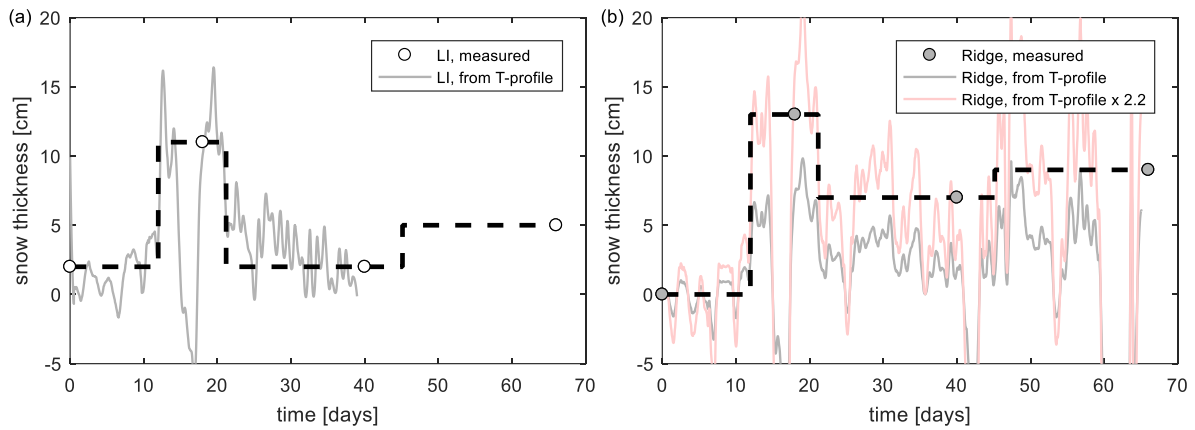
Figure 7. Snow thickness above level ice (a) and consolidated layer (b) vs time.

The analytical model allows accurately predicting level ice growth (Figure 8a). Top surface freezing is not included in the model. Based on salinity profiles at visit 1 and 4 (Figure 5a and b), around 4 cm was formed above the initial top surface.

Level ice thickness from direct measurements at visit 4 was 99 cm, while our analytical model predicted the thickness of 95 cm (Figure 8a). The numerical model result was 2 % larger than of analytical. The observed consolidated layer thickness was 120 cm, and 116 cm from the analytical model (Figure 8b). The numerical model result was 122 cm.

At the visit 4 salinity, density and temperature of level ice and consolidated layer were measured, giving 8 % of liquid volume fraction (Figure 5b) and 2 % of gas volume fraction. The analytical model final liquid volume fraction was 9 % for both level ice and consolidated layer.

Table 1. Evolution of the main level ice and consolidated layer properties

Property	Visit number			
	1	2	3	4
Number of LI/CL cores	3/0	0/2	0/4	1/12
Consolidated layer min. [m]	0.00	0.78	0.97	1.00
Consolidated layer avg. [m]	-	0.96	1.13	1.20
Level ice thickness [m]	0.50	0.65	0.82	0.99
Ridge snow thickness [m]	0.00	0.13	0.07	0.09
Level ice snow thickness [m]	0.02	0.11	0.02	0.05
Consolidated layer salinity [ppt]	3.8	4.2	3.8	4.1
Level ice salinity [ppt]	3.8	-	-	4.6
FDD [°d]	705	915	1228	1421

The analytical model also predicts the final consolidated layer thickness quite precise. Higher thickness values from drilling during visit 2 can be explained by the lack of a number of performed cores. Higher consolidation values from temperature profile are coming from the method overestimation when the temperature information is derived from the ridge block, not from the void. This effect is eliminated at the time of visit 4 because the consolidated layer reached the block bottom in the vertical profile of the thermistor (Figure 8b).
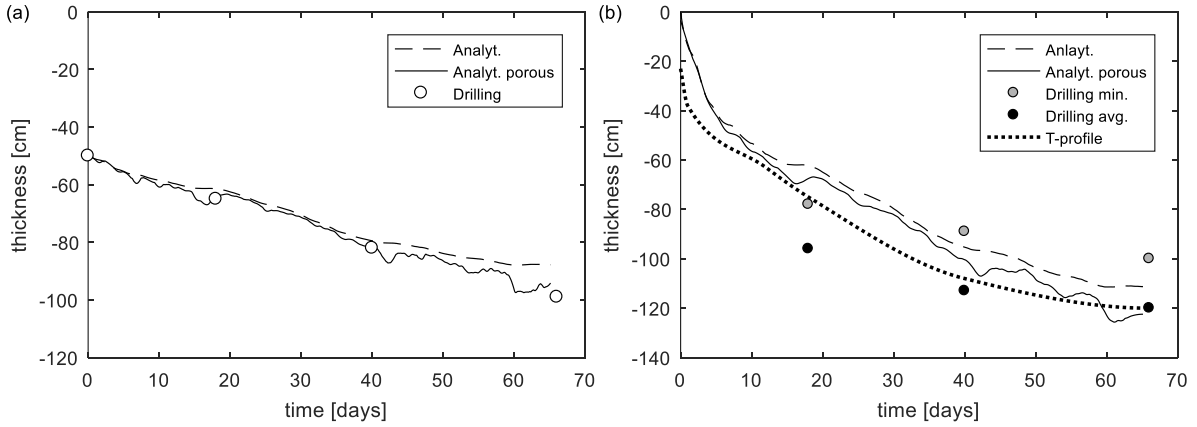
Figure 8. Level ice (a) and consolidated layer (b) thickness vs time.

The top surface temperature of ice ridges strongly depends on its elevation. Comparison of experimental heat fluxes through the sail of 15 cm height, through the consolidated layer and through level ice is presented in Figure 9a. The average heat flux in the sail was 1.8 times larger than in the consolidated layer. The analytical model is overestimating average heat flux in the consolidated layer only by 1.6 % (Figure 9b).
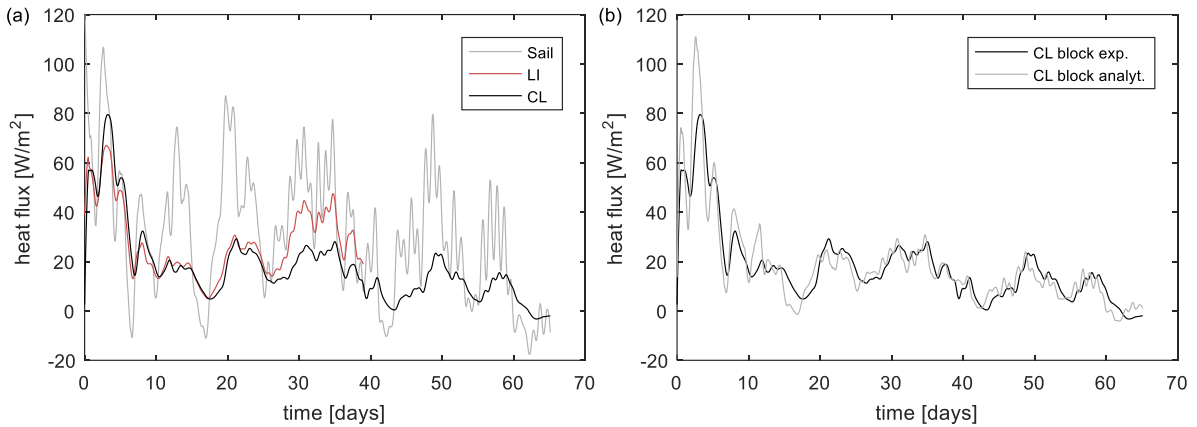

Figure 9. Vertical heat fluxes in ridge sail, consolidated layer and level ice (a) and comparison of heat fluxes in ridge block from experiment and from the analytical model (b).

Results of in-situ and laboratory uniaxial compression experiments, performed during visits 2, 3 and 4, are presented in Figure 10.
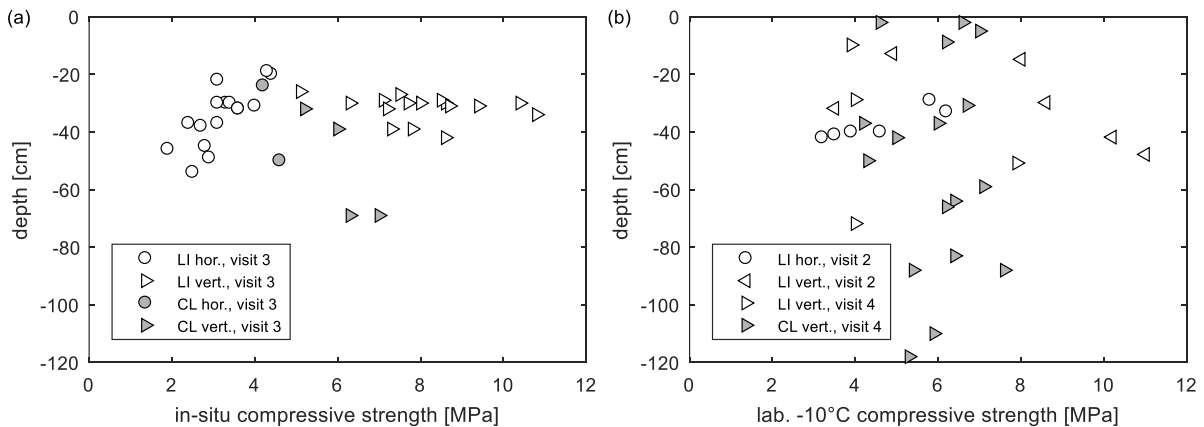

Figure 10. Uniaxial compressive strength for in-situ (a) and -10°C (b) temperatures vs depth.

In-situ during visit 3 average compression strength of horizontal level ice samples was 3.2 MPa, and 8.1 MPa for vertical level ice samples. Horizontal samples from consolidated

layer had the strength of 4.4 MPa, and 6.1 MPa for vertical samples from the consolidated layer.

In laboratory conditions at the temperature of around -10°C, the average strength of horizontal level ice samples was 4.5 MPa at visit 2, vertical strength was 7.7 MPa at visit 2 and 5.0 MPa at visit 4. Vertical consolidated layer strength was 5.9 MPa.

The strength of level ice for visit 2 was measured in different directions for horizontal samples: for EW direction it was 6.0 MPa, for NS it was 3.4 MPa, for 45° to NS it was 4.2 MPa.

The samples from the ridge had a much higher percentage of failures in a ductile way in contrast to level ice.

DISCUSSION

The increasing trend of level ice salinity can be explained by the presence of approximately 12 cm thick part of snow ice at the beginning of the experiment. The final level ice salinity profile shows that around 4 cm of ice was formed on the top during the experiment (Figure 4b). The decreasing portion of less saline snow ice is explaining the increase of level ice salinity with time.

Slightly lower ridge salinity in comparison to level ice can be explained by stronger ice desalinization after warming during initial phase according to the brine dynamics model by Griewank and Notz (2013). At the same time, according to Kovacs (1997), ice salinity depends on the ice growth rate. Vertical heat fluxes were almost equal in the consolidated layer and in level ice during the first 25 days (Figure 9a), when upper 70 cm of the consolidated layer was formed. Ridge multi-directional desalinization process requires further investigations.

Strength relations of consolidated layer and level ice in the presented experiment are in a good agreement with the results from Shafrova and Høyland (2008).

Høyland (2002) described large errors of consolidated layer thickness measurements performed by drilling and by temperature profile analysis. Obviously, at the same vertical core, thickness from temperature profile cannot be higher than from drilling. Meanwhile, temperature profiles from the ridge voids and ridge blocks are different due to the presence of strong horizontal fluxes in ridges. It is important to mention that any ridge solidification model describes new ice formation in the ridge voids. It means that the result of such a model should correspond to the minimum consolidated layer thickness, which can be obtained from drilling or from temperature profile in the ridge void. It was found from numerical modelling that thickness of consolidated layer obtained from ridge temperature profile can differ from the thickness of newly formed ice, and this difference is scale dependent.

At the level of minimum consolidated layer thickness, the temperature in the surrounding ice blocks can be significantly colder depending on their distance from the block center. Thermistor string for the described experiment was placed in the ice block. From the Figure 8b it can be seen, that thickness values from the temperature profile are always approximately 15 cm larger than of analytical solution, while vertical heat fluxes in fully consolidated part are almost equal for both the experiment and the model.

An example of the modelled temperature profile from the ridge block and void is shown in Figure 11. For that specific example from numerical simulation air ambient temperature is -15°C, sail height is 15 cm, and there is no snow. Under the assumption of a linear temperature profile, the estimated thickness in the block is 14 cm larger than in the ridge void, similar to the experimental observations.
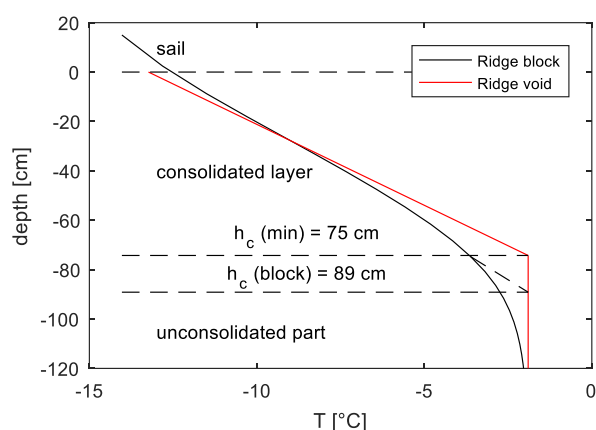
Figure 11. Ridge temperature profiles for block and void from the numerical simulation.

The heat fluxes in level ice and the consolidated layer below water level were almost equal during the first 25 days of the experiment when the snow thickness above both types of ice was in the same range (Figure 9a). Level ice thickness and corresponding thermal resistance were higher only during the first 12 days (Figure 6a). It shows the importance of coupling of air convection and conduction through snow and ice. At the same time, heat flux through the sail was 1.8 times higher than through the underwater consolidated layer. This difference corresponds to the difference in snow thermal resistance for the ridge and level ice of 2.2. The possible explanation for this difference in vertical fluxes is the existence of significant horizontal fluxes in the sail through its lateral surfaces. For the sail height of 15 cm and the block side length of 50 cm, the ratio of the area and the sail vertical projection is also equal to 2.2.

The question for future investigations is how the top flux difference from 1D and 3D models can affect the rate of ridge solidification and how it can be affected by the presence of snow.

CONCLUSIONS

This paper provides details of artificial ridge preparation and temporal investigations of its morphological, thermal and mechanical parameters. It was shown that the artificial ridge is providing sufficient information for accurate growth prediction and validation of ridge solidification models. It was confirmed that the top ridge surface temperature could be predicted only considering sail morphology.

One-dimensional analytical model using thermal resistance concept was described and applied for both level ice and ridge consolidation. A detailed description of the model application for usage with meteorological data and basic parameters from several visits of the experimental site was provided. It was shown that the ice growth for both saline level ice and the consolidated layer of saline ice ridges has significant differences from the fresh ice growth, and that accurate thickness prediction is only possible considering sea ice micro-porosity. The described analytical model can predict heat fluxes inside the consolidated layer quite accurately allowing a fast analysis of experimental data or predictions.

It was observed in the experiment, that the temperature profile could give overestimated values of consolidated layer thickness depending on the profile location. Potential reasons were described and confirmed with both experiment and numerical simulations.

REFERENCES

Adams, C. M., French D.N. and Kingery W. D., 1960. Solidification of sea ice. *Journal of Glaciology*, 3(28), 745-760.

Ashton G.D., 1989. Thin Ice Growth. *Journal of Water Resources Research*. Vol. 25, No. 3, pp. 564–566.

Blanchet, D., 1998. Ice loads from first-year ice ridges and rubble fields. *Canadian Journal of Civil Engineering*. 25 (2), pp. 206–219.

Cox, G.F.N. & Weeks, W.F., 1983. Equations for determining the gas and brine volumes in sea-ice samples. *Journal of Glaciology*, pp. 306–316.

Ervik, Å., Nord T.N., Høyland, K. V. Samardzija I., Li, H., 2019. Ice-ridge interactions with the Norströmsgrund lighthouse: Global forces and interaction modes. *Cold Region Science and Technology*, 158, pp. 195-220.

Griewank, P. J. & Notz, D., 2013. Insights into brine dynamics and sea ice desalination from a 1-D model study of gravity drainage. *Journal of Geophysical Research: Oceans*, 118(7), pp. 3370–3386.

Høyland, K.V., 2002. Consolidation of first-year sea ice ridges. *Journal of Geophysical Research*, 107 (C6), 15_1-15_7.

Kovacs, A., 1997. *Sea ice. Part 1: Bulk salinity versus ice floe thickness*. CRREL Rep. 96-7.

Leppäranta, M. & R. Hakala, 1992. The structure and strength of first-year ridges in the Baltic Sea. *Cold Region Science and Technology*, 92, pp. 295– 311.

Leppäranta, M., Lensu, M., Kosloff, P., Veitch, B., 1995. The life story of a first-year sea ice ridge. *Cold Region Science and Technology*, 23 (3), pp. 279–290.

Marchenko, A. & Morozov, E., 2013. Asymmetric tide in Lake Vallunden (Spitsbergen). *Nonlinear Processes in Geophysics*, 20, pp. 935-944.

Notz, D., 2005. *Thermodynamic and Fluid-Dynamical Processes in Sea Ice*. Ph.D. thesis, Univ. of Cambridge, Cambridge, U. K.

Petrich, C., Langhorne P. J., & Sun Z. F., 2007. Formation and structure of refrozen cracks in land-fast first-year sea ice. *Journal of Geophysical Research: Atmospheres*, 112:C04006.

Salganik, E. & Høyland, K. V., 2018. Thermodynamics and Consolidation of Fresh Ice Ridges for Different Scale and Configuration. *Proceedings of the 24th IAHR International Symposium on Ice*, Vladivostok, Russia, pp. 304-311.

Schwerdtfeger, P., 1963. The thermal properties of sea ice. *Journal of Glaciology*. 789–807.

Shafrova, S. & Høyland, K.V., 2008. Morphology and 2D spatial strength distribution in two Arctic first-year sea ice ridges. *Cold Region Science and Technology*, 51 (1), pp. 38–55.

Shestov, A. & Høyland, K. V. and Ervik, Å., 2018. Decay phase thermodynamics of ice ridges in the Arctic Ocean. *Cold Region Science and Technology*, 152, pp. 23-34.

Stefan, J., 1891. Uber die Theorie der Eisbildung, insbesondere uber die Eisbildung im Polarmeere, *Annalen der Physik und Chemie*, 42, pp. 269-286.

Timco, G. W. & L. E. Goodrich, 1988. Ice rubble consolidation. *9th International Symposium on Ice, International Association of Hydraulic Engineering*, Sapporo, Japan.

World Meteorological Organization, 1970. *WMO sea ice nomenclature* (supplement No 5.1989). Technical Report MO No. 259.TP.145. World Meteorological Organization, Geneva, Switzerland.